Minireview

Submolecular resolution of single macromolecules with atomic force microscopy

Daniel M. Czajkowsky, Zhifeng Shao*

Department of Molecular Physiology and Biological Physics and Biophysics Program, University of Virginia School of Medicine, Charlottesville, VA 22908, USA

Received 15 April 1998

Abstract The intrinsically high signal-to-noise ratio of atomic force microscopy (AFM) permits structural determination of individual macromolecules to, at times, subnanometer resolution directly from unprocessed images, avoiding the conditions and possible consequences of averaging over an ensemble of molecules. In this article, we will review some of the most recent achievements in imaging single macromolecules with AFM.

Key words: Atomic force microscopy; Individual molecule; Structure; Imaging methods

1. Introduction

Much of our knowledge about the structures of biological macromolecules has been generated by X-ray diffraction and electron microscopy (EM). These methods, however, have an intrinsically low signal-to-noise ratio, and thus require the signal obtained from an ensemble of molecules to be averaged. For the most part, this entails analysis of only those macromolecules which can be crystallized, although single particle averaging in EM is beginning to show promising results [1,2]. Still, by averaging over the ensemble, one might not be able to detect characteristics of an individual macromolecule, such as isoenergetic conformational substates [3], or one might inadvertently impose structural features such as size or symmetry onto the molecule that are not immediately apparent in the raw data [4]. For this reason, there has been a great deal of effort in the development of techniques that can directly resolve the structures of individual biological macromolecules. Foremost among these has been atomic force microscopy (AFM) [5].

Early on, the intense interest in AFM in biology emerged from a recognition that this method could resolve the surface features of heterogeneous samples under a variety of conditions, including in buffer solutions, giving rise to the possibility to directly image biological complexes in action [6]. Although there are a few examples where dynamic complexes were observed with AFM [6–11], many samples, whether catalytically active or not, were found either to be too weakly adsorbed to a substrate, too soft, or to fluctuate too greatly for high resolution imaging, raising concerns about AFM as a practical structural tool. Recent improvements in imaging techniques and sample preparation procedures, however, have produced results which demonstrate that AFM is indeed capable of detecting, to submolecular resolution, the surface features of a remarkable variety of individual macromolecules. Close-packed samples that tightly adsorb to mica have been imaged up to subnanometer resolution in solution [10–21]. Where a sample has been found to be too delicate for the applied force of the scanning tip, the application of cross-linking agents has been shown to increase its mechanical strength, enabling the resolution of, in one case [19], secondary structures. If either adhesion to a substrate or sensitivity to the probe force is still too significant a problem, imaging at cryogenic temperatures has proven to be, to a remarkable degree, generally applicable [22–24].

In this article, we will briefly review some of the most recent achievements obtained by imaging single macromolecules at a high resolution with AFM and cryo-AFM, with particular emphasis on those instances where submolecular details could be directly resolved from the unprocessed image. Readers interested in a detailed description of the technique may consult appropriate reviews elsewhere [9,25,26].

2. Soluble proteins

By far the most popular substrate for biological AFM studies is the atomically smooth surface of muscovite mica. Although the mechanism by which macromolecules adsorb to this substrate still remains poorly understood [27], a large number of samples, from proteins to phospholipid bilayers, adhere tightly to this surface, albeit usually under a limited range of ionic strength [7], if not composition [28]. One of the most readily identifiable macromolecules with AFM is the pentameric B-subunit from cholera toxin [18]. This 60-kDa oligomer binds to its ganglioside receptor, G_{M1}, on the surface of intestinal epithelial cell membranes, and once endocytosed, enables the catalytic A-subunit of this toxin (by a mechanism still not fully known [29]) to enter the cytoplasm where it ADP-ribosylates the G-protein G_s [30]. The upper panel of Fig. 1a is an image, obtained (as all examples presented in this review) using the contact mode [9,25,26], of a population of B-oligomers, each about 6 nm in outer diameter with a 1-nm pore, adsorbed to mica in solution. The resolution of this non-crystalline yet close-packed sample at this large scan size is nonetheless sufficient to discern not only several clear examples of a pentameric stoichiometry, but also oligomers with less than five subunits. A smaller scan size image (see the lower panel of Fig. 1a) shows more clearly a range of different stoichiometries (predominantly pentamers), in addition to one oligomer (see arrow) which appears to be splayed open, perhaps indicating a strain in this oligomer prior to the break in the intersubunit contact.

*Corresponding author. Fax: (1) (804) 9821616.
E-mail: zs9q@virginia.edu

PII: S0014-5793(98)00461-X

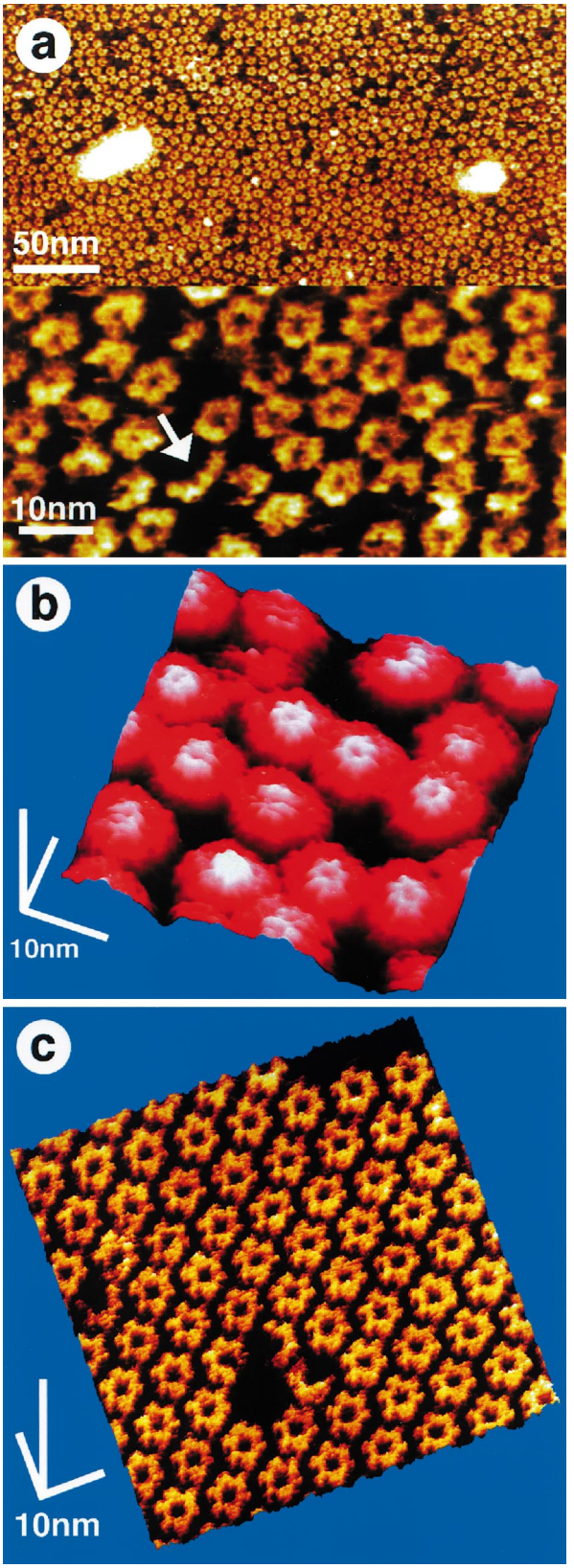

Fig. 1. Contact-mode AFM images of soluble and membrane proteins, obtained in solution at room temperature. a: The B-oligomer of cholera toxin on mica. The upper panel shows that the features routinely revealed in AFM images of this oligomer (namely, the pentameric stoichiometry and the 1-nm pore) can be clearly discerned even at this larger scan size. Also apparent in this image are several oligomers with less than five subunits. The lower panel is a higher resolution image, showing in greater detail several pentamers, as well as some smaller oligomers, including one (see arrow) that appears to be splayed open, perhaps indicating a strain in the molecule prior to the break in the intersubunit contact. b: The co-chaperonin GroES, adsorbed to mica in the presence of Mg^{2+}. The crown-like nature of this heptamer is clearly revealed in this unprocessed image. This structure was subsequently found to be consistent with the structure determined from X-ray diffraction. Comparison with the X-ray structure indicated that each radial spoke atop the crown is an 8-Å wide β-turn. c: Staphylococcal αHL oligomers in a supported bilayer. In contrast to the heptameric stoichiometry recently elucidated by X-ray diffraction of the oligomer formed in deoxycholate micelles, unprocessed images of αHL oligomers in a phospholipid bilayer clearly revealed only hexamers, demonstrating a previously unknown polymorphism in subunit stoichiometry of αHL. The observation of stable oligomers with less than six subunits suggests that there may be arc-shaped oligomers of αHL, as there are with other toxins, that can nonetheless form a pore.
←

A second example of a soluble protein that interacts with sufficient strength to mica (in this case in the presence of Mg^{2+}) is the co-chaperonin, GroES [19]. This oligomer complexes with the tetradecamer GroEL (also imaged to high resolution with AFM [20]) to facilitate protein folding in an ATP-dependent manner [31]. An early EM model of GroES [32] depicted a featureless ring, 7–8 nm in diameter, whereas a more recent EM study [33] produced a structure with seven radial subunits, surrounding a 2.6-nm pore. The close-packed oligomers in this unprocessed AFM image (Fig. 1b) clearly reveal a crown-like heptamer, a structure which was subsequently found to be consistent with, in topography and dimension, the structure determined by X-ray diffraction [34,35]. To obtain this structure, fixation with glutaraldehyde was found to ease the resolution of the uppermost region as seven radial spokes. Comparison of this structure with that of the X-ray model revealed that each of the radial spokes is an 8-Å wide β-turn, indicating that secondary structural elements can be directly detected with AFM. Other examples of secondary structures resolved with AFM include β-sheets in the protein coat of the gas vesicle of *Anabaena flos-aquae* [17] and a flexible cytoplasmic loop of the membrane protein, bacteriorhodopsin [11].

A common characteristic of these high resolution images is the close-packed nature of the sample, which may decrease the tip-pressure applied to any one macromolecule [26]. As such, two-dimensional crystals are among the most suitable specimens for AFM imaging, as demonstrated by Engel and coworkers [9–14]. One recent example [13] that produced astonishing images is the two-dimensional crystal of the oligomeric bacteriophage ϕ29 connector. Based on high resolution surface features of both ends of this connector, Müller et al. were able to refine a previous model determined from EM [13].

3. Membrane proteins

A natural choice of sample for AFM investigations is that group of macromolecules which are essentially confined, in their native environment, to two dimensions: the membrane proteins. Successful efforts include gap junctions [16], bacteriorhodopsin [11,12], the HPI-layer [10], aquaporin [14], OmpF [15], and the B-subunit of cholera toxin [18]. (A more thorough review may be found elsewhere in this issue.)

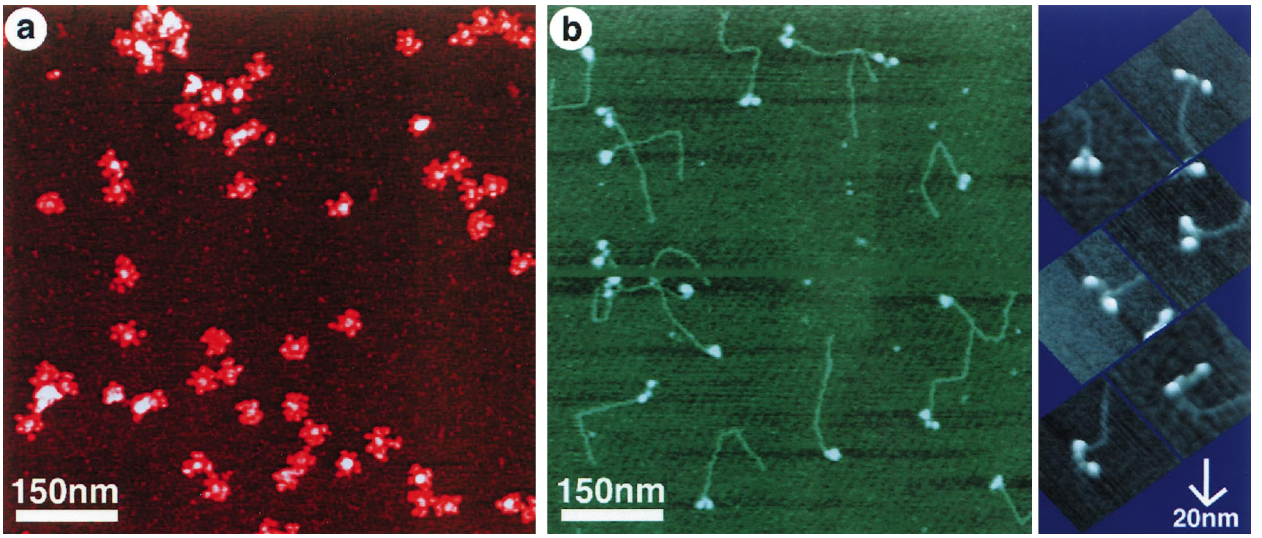

Fig. 2. Cryo-AFM images of macromolecular proteins adsorbed on mica. a: The oligomeric immunoglobulin complex, IgM. In contrast to a previous model that depicted this complex as a flat pentamer, cryo-AFM images revealed a prominent, central protrusion. b: Non-phosphorylated smooth muscle myosin. The characteristic bi-lobed head region and kinked coiled-coil tail are clearly discerned in this image. The resolution in these cryo-AFM images is sufficiently high to enable the detection of the two separate regions, the motor and regulatory domains, within each myosin head (see isolated images, at a higher resolution, on the right).

One of the more intriguing membrane proteins studied recently is the toxin staphylococcal α-hemolysin (αHL), which is secreted as a 33-kDa water-soluble monomer that converts into a pore-forming oligomer upon contact with the plasma membrane. This oligomer was long believed to be a hexamer based on a range of biophysical and biochemical experiments [36]. However, recent X-ray crystallography of the oligomer formed in deoxycholate micelles clearly revealed a heptameric stoichiometry, leading to the suggestion that the previous techniques were of insufficient resolution to assess subunit stoichiometry [37]. Injection of the water soluble monomers into the solution covering a supported bilayer produced large regions of close-packed oligomers, suitable for AFM imaging [21]. The unprocessed image in Fig. 1c clearly indicates that each individual αHL oligomer in this membrane is a hexamer. Analysis of the lattice parameters (as well as gel electrophoresis) supported this observation of an oligomer smaller than the heptamer detected in X-ray diffraction. Hence, there appears to be a previously unknown polymorphism in the subunit stoichiometry of the αHL oligomer. In addition, it is clear from this image (Fig. 1c) that there are oligomers with less than six subunits associated with the bilayer, which suggests that there may be arc-shaped oligomers of αHL, as there are with other toxins [38], which can nonetheless form a pore.

4. Cryo-AFM

Although technical developments for improved imaging in solution by AFM are likely not yet exhausted, there will probably always be macromolecules or large complexes, which are too soft or fluctuate too greatly to be imaged in solution. It was thus desired that a system be developed which enables imaging of biological samples at cryogenic temperatures, where the mechanical strength of individual molecules could be greater and the thermal fluctuations reduced [22,23]. From among several proposed systems, simply suspending an AFM above a pool of liquid nitrogen within a dewar proved to be the most successful, producing even atomic resolution of NaCl crystals [22]. With this system, direct imaging of isolated macromolecules under a range of applied forces demonstrated that the mechanical stability of individual molecules was indeed enhanced, perhaps by up to 10^3–10^4 times [22]. Several complexes, such as immunoglobulins, which are notoriously difficult to be imaged by AFM in solution, have been easily visualized in the cryo-AFM. One such example is the oligomeric immunoglobulin, IgM, composed of five IgE-like subunits and a small 17-kDa J-chain. Early models from EM [39] depict an essentially planar complex, with the F_c domains of the IgE-like subunits connected at a central location, thought to be the site of J-chain binding as well. Although cryo-AFM images from aged samples of IgM showed some flat pentamers, images from freshly prepared samples (Fig. 2a) revealed a more compact oligomer with a pronounced central protrusion, which is too large to be only the J-chain. It is possible that the F_c domains in this complex protrude from the plane defined by the F_{ab} domains, and that after some degradation, the center collapses.

Another example of a macromolecule that has been difficult to image in solution by AFM is the molecular motor, myosin [40]. Cryo-AFM images (Fig. 2b) of smooth-muscle myosin are of sufficient resolution not only to clearly resolve the two heads and the coiled-coil tail, but also to reveal the two domains (motor and regulatory) within a myosin single head [24]. An interesting set of images [24] was produced from myosin molecules prepared from a lower ionic strength: the coiled-coil tails were observed to unwind, indicating a strong destabilizing electrostatic component in the interaction between the two α-helices.

Submolecular details of other heterogeneous samples observed with cryo-AFM include surface corrugations on red blood cell membranes [22,23], monomers of actin within individual actin filaments and bundles (unpublished observations), and sub-nucleosomal components from purified chromatin (unpublished observations).

5. Future perspective

The resolution that AFM might ultimately achieve will probably never rival the atomic resolution possible with X-ray diffraction and EM. Even with further technical improvements, AFM will still be limited to the generation of only the tip-accessible surface of the macromolecular complex. The unique strength of AFM in structural biology will, however, always be its ability to directly reveal submolecular surface features, whether in solution or at cryogenic temperatures, of macromolecular complexes or of heterogeneous populations of such complexes that cannot be readily crystallized. As presented above, with some samples AFM can be used to generate unambiguous data about the stoichiometry (or range of stoichiometries) and the disposition of subunits within an individual molecular complex. It might be thus possible to determine the structures of heterogeneous, multi-molecular complexes by first determining the structure of the individual components by X-ray crystallography, and then fitting these into the high resolution topographical envelopes of the assembled complexes generated by AFM, in a similar manner as in EM. From this, it may be possible to then use AFM to directly visualize submolecular rearrangements of the ensemble of complexes under different biochemically or biologically characterized conditions. If the sample proves too soft or flexible, intermediates may still be observed by trapping the complex with particular ligands, chemical fixation, or rapid freezing. In this way, AFM may thus provide a direct link from the atomic details to the range of conformations, associated with a particular biological function, that are adopted by a heterogeneous population of macromolecular complexes.

Acknowledgements: We thank Y. Zhang for the images of IgM and myosin, and Dr. J. Mou for the image of GroES. We also thank Drs. A.P. Somlyo, A.V. Somlyo, P.K. Hansma, and G. Lorimer for many stimulating discussions. Work presented here has been supported by grants from the National Institutes of Health (RO1-RR07720 and PO1-HL48807) and the American Heart Association.

References

[1] Agrawal, R.K., Penczek, P., Grassucci, R.A., Li, Y., Leith, A., Nierhaus, K.H. and Frank, J. (1996) Science 271, 1000–1002.
[2] Stark, H., Orlova, E.V., Rinke-Appel, J., Jünke, N., Mueller, F., Rodina, M., Wintermeyer, W., Brimacombe, R. and van Heel, M. (1997) Cell 88, 19–28.
[3] Frauenfelder, H., Sligar, S.G. and Wolynes, P.G. (1991) Science 254, 1598–1603.
[4] Ludwig, D.S., Ribi, H.O., Schoolnik, G.K. and Kornberg, R.D. (1986) Proc. Natl. Acad. Sci. USA 83, 8585–8588.
[5] Binnig, G., Quate, C.F. and Gerber, Ch. (1986) Phys. Rev. Lett. 56, 930–933.
[6] Drake, B., Prater, C.B., Weisenhorn, A.L., Gould, S.A.C., Albrecht, T.R., Quate, C.F., Cannell, D.S., Hansma, H.G. and Hansma, P.K. (1989) Science 243, 1586–1589.
[7] Bezanilla, M., Drake, B., Nudler, E., Kaahlev, M., Hansma, P.K. and Hansma, H.G. (1994) Biophys. J. 67, 2454–2459.
[8] Kasas, S., Thomson, N.H., Smith, B.L., Hansma, H.G., Zhu, X., Guthold, M., Bustamante, C., Kool, E.T., Kashlev, M. and Hansma, P.K. (1997) Biochemistry 36, 461–468.
[9] Bustamante, C., Rivetti, C. and Keller, D.J. (1997) Curr. Op. Struct. Biol. 7, 709–716.
[10] Müller, D.J., Baumeister, W. and Engel, A. (1996) J. Bacteriol. 178, 3025–3030.
[11] Müller, D.J., Büldt, G. and Engel, A. (1995) J. Mol. Biol. 249, 239–243.
[12] Müller, D.J., Schabert, F.A., Büldt, G. and Engel, A. (1995) Biophys. J. 68, 1681–1686.
[13] Müller, D.J., Engel, A., Carrascosa, J.L. and Vélex, M. (1997) EMBO J. 16, 2547–2553.
[14] Walz, T., Tittmann, P., Fuchs, K.H., Müller, D.J., Smith, B.L., Agre, P., Gross, H. and Engel, A. (1996) J. Mol. Biol. 264, 907–918.
[15] Schabert, F.A., Henn, C. and Engel, A. (1995) Science 268, 92–94.
[16] Hoh, J.H., Sosinsky, G.E., Revel, J.-P. and Hansma, P.K. (1993) Biophys. J. 65, 149–163.
[17] McMaster, T.J., Miles, M.J. and Walsby, A.E. (1996) Biophys. J. 70, 2432–2436.
[18] Mou, J., Yang, J. and Shao, Z. (1995) J. Mol. Biol. 248, 507–512.
[19] Mou, J., Czajkowsky, D.M., Sheng, S., Ho, R. and Shao, Z. (1996) FEBS Lett. 381, 161–164.
[20] Mou, J., Sheng, S., Ho, R. and Shao, Z. (1996) Biophys. J. 71, 2213–2221.
[21] Czajkowsky, D.M., Sheng, S. and Shao, Z. (1998) J. Mol. Biol. 276, 325–330.
[22] Han, W., Mou, J., Sheng, S., Yang, J. and Shao, Z. (1995) Biochemistry 34, 8215–8220.
[23] Zhang, Y., Sheng, S. and Shao, Z. (1996) Biophys. J. 71, 2168–2176.
[24] Zhang, Y., Shao, Z., Somlyo, A.P. and Somlyo, A.V. (1997) Biophys. J. 1308–1318.
[25] Engel, A., Schoenenberger, C.-A. and Müller, D.J. (1997) Curr. Op. Struct. Biol. 7, 279–284.
[26] Shao, Z., Mou, J., Czajkowsky, D.M., Yang, J. and Yuan, J.-Y. (1996) Adv. Phys. 45, 1–86.
[27] Müller, D.J., Amrein, M. and Engel, A. (1997) J. Struct. Biol. 119, 172–188.
[28] Hansma, H.G. and Laney, D.E. (1996) Biophys. J. 70, 1933–1939.
[29] Hazes, B. and Read, R.J. (1997) Biochemistry 36, 11051–11054.
[30] Spangler, B.D. (1992) Microbiol. Rev. 56, 622–647.
[31] Lorimer, G.H. (1994) Structure 2, 1125–1128.
[32] Harris, J.R., Plückthun, A. and Zahn, R. (1994) J. Struct. Biol. 112, 216–230.
[33] Tsuprun, V., Rajagopal, B.S. and Anderson, D. (1995) J. Struct. Biol. 115, 258–266.
[34] Mande, S.C., Mehra, V., Bloom, B.R. and Hol, W.G. (1996) Science 271, 203–207.
[35] Hunt, J.F., Weaver, A.J., Landry, S.J., Gierasch, L. and Deisenhofer, J. (1996) Nature 379, 37–45.
[36] Bhakdi, S. and Tranum-Jensen, J. (1991) Microbiol. Rev. 55, 733–751.
[37] Song, L., Hobaugh, M.R., Shustak, C., Cheley, S., Bayley, H. and Gouaux, J.E. (1996) Science 274, 1859–1866.
[38] Bhakdi, S., Bayley, H., Valeva, A., Walev, I., Walker, B., Weller, U., Kehoe, M. and Palmer, M. (1996) Arch. Microbiol. 165, 73–79.
[39] Parkhouse, R.M., Askonas, B.A. and Dourmashkin, P.K. (1970) Immunology 18, 575–584.
[40] Hallett, P., Offer, G. and Miles, M.J. (1995) Biophys. J. 68, 1604–1606.